

Formulations for the scattering properties of suspended sandy sediments for use in the application of acoustics to sediment transport processes.

Peter D. Thorne^{1*} and Ramazan Meral²

1. Proudman Oceanographic Laboratory

Joseph Proudman Building

6 Brownlow Street

Liverpool, L3 5DA, UK

2. Kahramanmaras University

Faculty of Agriculture

Department of Agricultural Structures and Irrigation

Kahramanmaras

Turkey

*pdt@pol.ac.uk corresponding author

Key words: Sediments, transport, acoustics, scattering, attenuation, instrumentation

P. D THORNE AND R MERAL 2008

Formulations for the scattering properties of sandy sediments for use in the application of acoustics to sediment transport. *Continental Shelf Research*, 28, 309-317.

Abstract

Multi-frequency acoustics backscattering has been used for over a decade, to quantitatively measure profiles of suspended sediment particle size and concentration, in the bottom 1-2 m above the seabed. Central to obtaining the sediment parameters from the backscattered signal is a description of the scattering characteristics of the particles in suspension. Therefore, formulations are required for the attenuation and backscattering properties of the suspended particles with size and acoustic frequency. There is no single formulation for these scattering properties and different researchers have used somewhat different expressions. However, these expressions are all based on a variation of sphere scattering, modified to fit available scattering data. Here we bring together all the published data on acoustic backscattering and attenuation by suspensions of sandy sediments. The aim is to provide coastal scientists, who use acoustics for sediment transport measurements, with simple expressions which best represent the observed scattering properties of sandy sediments.

I Introduction

In recent years acoustic instrumentation has been increasingly used to measure non-intrusively, co-located and simultaneously, near-bed profiles of the flow, the suspended sediments and the bed forms, Thorne and Hanes 2002. Here we highlight the use of multi-frequency acoustic backscattering systems, ABS, for the measurement of particle size and concentration over sandy beds. To extract the suspended sediment parameters from the backscattered signal requires an inversion to be conducted on the signal. At the kernel of this inversion is a description of the scattering properties of the particles in suspension. For suspensions composed of marine sands the individual grains are irregular in shape. At present there does not exist an exact solution to the general problem of scattering by irregularly shaped scatterers. Therefore the approach used to describe the scattering properties of suspensions of sandy sediments has been through direct measurement of their scattering properties and the utilization of sphere scattering models to interpret and represent the observations.

The ABS's currently in use typically operate at three frequencies in transceiver mode; that is the transmit transducers are also used as receivers (Crawford and Hay 1993, Thorne et al 2002, Vincent and Hanes 2002, Green et al 2004, Dohmen-Jassen and Hanes 2005). The frequencies are usually in the range 0.5 MHz – 5MHz and the aim is to use the differential scattering characteristics of the scatterers with frequency to establish the suspended particle size and concentration. Because ABS's are normally used in transceiver mode, it is the backscattering and attenuating characteristics of the suspended sediment which are required for the acoustic inversion. The relevant acoustic quantities are the backscatter form function, f , which describes the backscattering characteristics of the particles in suspension, and the normalized total scattering cross-section, χ , which describes the attenuating characteristics. Both are non-dimensional parameters and their origins and nomenclature come from the acoustic sphere scattering literature (Neubauer et al 1974). Appendix 1 provides a brief background on f and χ for readers not conversant with the acoustic scattering literature.

The sphere scattering approach, using the f and χ representation, was first adopted by Sheng and Hay 1988 to explain the sediment attenuation observations of Flammer 1962. They used a rigid mobile sphere model which compared reasonably well with the measurements and they also formulated a simple heuristic expression which also provided good agreement with the data. Other publications have adopted a similar approach (Hay and Sheng 1992, Crawford and Hay 1993, Thorne et al 1993, Schaafsma and Hay 1997, Thorne and Hanes 2002, Thorne and Buckingham 2004) and presented similar, though different expressions, related to particular data sets. In this study the objective was to bring together the published literature on acoustic scattering by suspensions of sandy sediments and irregularly shaped particles. The aim was to provide simple expressions for f and χ which compared well with all the data sets available and which can be used with a reasonable degree of confidence in the interpretation of ABS data collected above sandy sediments.

II Background to f and γ

If the phase of the backscattered signal from a suspension of sediments is randomly distributed between $0-2\pi$, then forinsonification by a piston transceiver, the backscattered signal from a multi-frequency ABS can be converted to concentration, M , and mean particle size, $\langle a \rangle$, (Sheng and Hay 1988, Hay 1991, Thorne et al 1993, Thorne and Hanes 2002) using

$$M = \left\{ \frac{V_{\text{rms}} \psi r}{k_s k_t} \right\}^2 e^{4r(\alpha_w + \alpha_s)} \quad (1)$$

$$k_s = \frac{\langle f \rangle}{\sqrt{\langle a \rangle \rho}}, \quad \alpha_s = \frac{3}{4r\rho} \int_0^r \frac{\langle \chi \rangle M}{\langle a \rangle} dr$$

The above expression assumes the attenuation over a range bin is not substantial (see Hay 1991). V_{rms} is the root-mean-square backscattered signal; this is an ensemble average over a number of backscatter returns. The ensemble is required because the individual backscattered signals are Rayleigh distributed (Libicki et al 1989, Thorne et al 1993). r is the range from the transceiver, ψ accounts for the departure from spherical spreading within the transducer nearfield, k_s represents the scattering properties of the sediments, ρ is the density of the sand grains in suspension, k_t is a system constant (see preceding companion paper, Betteridge et al 2007, for its measurement), α_w is attenuation due to water absorption and the other terms are given below.

$$\langle a \rangle = \int_0^{\infty} aP(a) da \quad (2)$$

$$\langle f(x_o) \rangle = \left\{ \frac{\int_0^{\infty} aP(a) da \int_0^{\infty} a^2 f(x)^2 P(a) da}{\int_0^{\infty} a^3 P(a) da} \right\}^{1/2} \quad (3)$$

$$\langle \chi(x_o) \rangle = \frac{\int_0^{\infty} aP(a) da \int_0^{\infty} a^2 \chi(x)P(a) da}{\int_0^{\infty} a^3 P(a) da} \quad (4)$$

Where a is the radii of the sediment grains in suspension, $P(a)$ is the probability size distribution of the grains and $x=ka$, where k is the wave number, $k=2\pi/\lambda$, λ is the wavelength of the sound in water and $x_o=k\langle a \rangle$. The variable x is non-dimensional and as will be seen below is an appropriate choice for describing the dependency of f and χ . As a step towards the evaluation of equation (1), equations (3) and (4) need to be calculated and this requires expressions for f and χ . The purpose of the present paper is to provide these expressions using all the presently available published data, so that coastal scientists can use them in a straightforward manner in the interpretation of ABS data.

Although there is no general solution to the scattering properties of irregularly shaped particles we can make some reasonable estimates for $x \ll 1$ and $x \gg 1$. For $x \ll 1$, the Rayleigh regime, the wavelength of the sound is much greater than the particle circumference and scattering is considered to be independent of the shape of the scatterer. Therefore one might anticipate spherical and irregularly shaped scatterers may have similar scattering characteristics. Rayleigh scattering for a sphere is given by (Clay and Medwin 1998)

$$f = 2x^2 \left[\frac{e-1}{3e} + \frac{g-1}{2g+1} \right] \quad (5a)$$

$$\chi = 2x^4 \left[\left(\frac{e-1}{3e} \right)^2 + \frac{1}{3} \left(\frac{g-1}{2g+1} \right)^2 \right] \quad (5b)$$

$e=E_1/E_0$ is the ratio of elasticity of sand grains (quartz) to water, $e=39$, and g is the ratio of density of the sand grains to water, $g=2.65$. Putting the values for e and g into equation (5) gives $f=1.17x^2$ and $\chi=0.26x^4$; these are particularly simple expressions. For $x \gg 1$, the geometric regime, the scattering cross-section is the particle's actual cross-section. There is a theorem (Hulst 1981, Chinnery et al 1997) that states that the geometric cross-section of a convex particle, averaged over all orientations, is equal to a quarter of the surface area of the particle. This is obviously the case for a sphere where the surface area is $4\pi a^2$ and the cross-sectional area is πa^2 . Since a sphere has the minimum surface area to volume, then it is expected that a particle of irregular shape, having a similar volume to a sphere, would have a larger surface area and hence a higher geometric and scattering cross-section. For a rigid sphere f and χ tend to a constant value of unity for $x \gg 1$ and therefore it might be reasonable to anticipate that for irregularly shaped particles f and χ would tend to a constant value somewhat greater than unity.

III Measurements and expressions

(i) Data sets

The first quantitative measurements which could be expressed in the form function formulation were collected on beach sands (Hay 1991). In this study a laboratory tank was filled with water and a suspended sediment jet was formed within the tank using a nozzle and pump arrangement. Acoustic backscatter measurements from the sediment jet were collected at 1.0 MHz, 2.25 MHz and 5.0 MHz, using three beach sands sieved into $\frac{1}{4}\phi$ size intervals and covering the radius range 58-231 μm . The results were compared with a rigid movable sphere with the density of quartz and a rigid sphere of infinite density. Later, Crawford and Hay 1993, applied curve fitting to the 1991 data set and a rational fraction was used to represent the observations. Following on from these measurements, broadband scattering from the sediment jet were carried out by He and Hay 1993. Data were collected on $\frac{1}{4}\phi$ sieved sand samples with mean radii of 57.75 μm , 98.0 μm and 162.5 μm , over the concentration range 0.35-5.66 kgm^{-3} and covering the frequency band 1.25-2.75 MHz in 0.2 MHz frequency intervals. The measurements were compared with rigid moveable sphere models which had the density of quartz. The data from the 1991 and 1993 studies were essentially consistent. Further measurements were reported by Thorne and Buckingham 2004 using sands collected from estuarine, beach and quarried locations. Observations were made in a sediment tower which generated a homogeneous suspension of sediments over a vertical range of about 1m. Data were collected over the particle radius range 45-390 μm in $\frac{1}{4}\phi$ sieved intervals. The acoustic frequencies used were 1.0 MHz, 2.0 MHz and 4.0 MHz. These data had values for f which were somewhat larger than those of Hay 1991 and He and Hay 1993 for $x > 1$. An enhanced smoothed sphere scattering model was used to interpret these measurements. Finally a series of measurements have been published on scattering by single irregularly shaped particles (Thorne et al 1995). Although the three previous data sets were from suspensions, it was not considered unreasonable to include the single particle scattering data in the present study. Measurements were collected on particles in the radius range 0.72-2.5 cm using a broadband system operating between 40-240 kHz and on particles

with radius between 0.15-0.2 cm using narrow band signals over the frequency range 0.6-2.2MHz.

The earliest useful published measurements on attenuation by suspensions of sandy sediments were reported over forty years ago by Flammer 1962. These data were used by Sheng and Hay 1988, to provide the first contemporary description of sediment scattering using sphere scattering models and a simple ‘high-pass’ heuristic model, which provided good agreement with the measurements. In the present work we have gone back to the original paper of Flammer, digitized the data reported in figure 3 and converted it to χ format. The measurements were collected over the radius range 26-455 μm , at six discrete frequencies between 2.5-25.0 MHz at a fixed concentration of 2.65 kgm^{-3} . Sheng and Hay 1988, in their table 2, also presented attenuation data from the measurements of Jansen (1978, 1979) and Schaaafsma and der Kinderen (1986), which we have also included here. The next data set is from the suspended sediment jet work (Hay 1991). Measurements were made over a range of concentrations nominally between $0.3\text{-}24 \text{ kgm}^{-3}$, using a selection of beach sands sieved into $\frac{1}{4}\phi$ size intervals, at frequencies of 2.25 MHz, 4.5 MHz and 5.0 MHz. Both a rigid sphere model with the density of quartz and the high-pass model were compared with the data. More recent (Shaafsmaa and Hay 1997) attenuation measurements were made on sandy sediments over the frequency range 2.25-100 MHz using $\frac{1}{4}\phi$ sieved radii of 11.5 μm , 24.5 μm , 49 μm and 98 μm . This data set showed a notable departure from the rigid mobile sphere model, with the attenuation of the suspensions of sandy sediment being higher than for spheres of a similar size for $x > 1$. A two parameter sphere scattering model was developed to explain these observations. Lastly, attenuation measurements were obtained from the gradient of the backscattered signal as part of the sediment tower study by Thorne and Buckingham 2004. The same enhanced smoothed sphere model was used to interpret these observations as was used with the form function measurements.

(ii) Data analysis

The data from the four studies on the form function for sandy suspensions and irregular shaped particles are shown in figure 1a. The data cover the range $x=0.2\text{-}30$. In general the

observations are similar in form for the different data sets; this is indicative that the non-dimensional scattering parameters used on the abscissa and the ordinate are appropriate for scattering by irregularly shaped particles. There is scatter in the data and this is considered to be associated with detailed differences in particle shape (Shaafsma and Hay 1997), different experimental procedures and experimental errors associated with the different data sets. As can be seen in figure 1a, between $x=0.2-2$ there is seen to be a relatively steady increase in the form function with x and with the trend being nominally consistent for the different data sets. Above the value of $x \approx 2$, the increase of f with x is no longer dominant and the data show somewhat less consistency. Above $x \approx 5$, the data available is only for single irregularly shaped scatters and the trend is nominally uniform with a possible slight reduction in form function as x increases. The complementary results for the measurements of the normalized total scattering cross-section are presented in figure 1b. Data were obtained between $x=0.3-50$. Again, as with the form function, the different data sets of the normalized total scattering cross-section generally follow a similar trend. The data show increasing values for χ with x up to a value of $x \approx 2$ and with a gradient steeper than was the case for the form function. Above $x \approx 2$ the rate of increase of χ with x is significantly reduced and at higher values of x , $x > 10$, χ appears to be nominally independent of x .

Plotted in figures 1a and 1b are linear regressions carried out on the logarithm of the data, for $x \leq 2.5$ and $x > 2.5$. The value of $x=2.5$ was chosen as the break point in the regression fitting because of the change in gradient at approximately this value of x . The regression lines were not fitted as theoretical matches to the data, but simply as a way of removing outliers from the general trends in the data. Data lying at a significant distance from the lines was considered as outside the general trends in the data. Figure 2 shows ratios of the measured values for f and χ divided by the calculated value from the linear regression fit to the data, f_r and χ_r . Values of this ratio between $1.5^{-1}-1.5$ were deemed as acceptable data. These boundaries retained most of the measurements, 92% for f , 81% for χ , while removing measurements which were outside the general body of the data sets.

Using the data within the 1.5^{-1} -1.5 specified boundaries; an averaging process was used to reduce the scatter in the data. Data between $x=0.1$ -1 were averaged over $x\pm 0.01$ intervals, data in the range $x=1$ -5 were average over $x\pm 0.1$ intervals, data in the range $x=5$ -20 were averaged into $x\pm 0.5$ intervals and above $x=20$ data were averaged into $x\pm 1$ intervals. These averaging intervals retained the form of the data and clarified the trends. The results are shown in figure 3, with error bars, derived by calculating the standard deviation of the f and χ values over the averaging intervals of x . Compared with figure 1 the trends in the data are somewhat clearer. In figure 3a the values for f steadily increase with x until $x\approx 1$, between $x=1$ -2 there seems to be a region of inflexion in the data, between $x=2$ -4 there is some variability in the data and above $x=10$ the form function is nominally constant in value. In figure 3b the values for χ are seen to increase rapidly with x up to $x\approx 2$, the gradient of the data then decreases with x , with χ becoming nominally independent of x for $x>10$.

(iii) Expressions for f and χ

To represent the measurements, formulae were derived on a heuristic basis and following procedures presented in previous publications (Sheng and Hay 1988, Crawford and Hay 1993, Thorne et al 1993, Thorne and Hanes 2002). Asymptotic constraints were imposed such that for $x\ll 1$, the Rayleigh regime, $f \propto x^2$ and $\chi \propto x^4$ and for $x\gg 1$, the geometric regime, f and χ were constant. For the form function the expression used was

$$f = \frac{x^2 \left(1 - \varphi_1 e^{-((x-x_1)/\zeta_1)^2} \right) \left(1 + \varphi_2 e^{-((x-x_2)/\zeta_2)^2} \right)}{1 + \delta_1 x^2} \quad (6)$$

For $x\ll 1$, the two bracketed terms tend to a constant, c_0 , hence $f=c_0 x^2$. For $x\gg 1$, $f=1/\delta_1$ which is constant and independent of x . The first bracket containing the exponential introduces the inflexion region around $x=1$ -2. Physically this is associated with a back and forth movement of the particles in the water due to the propagating acoustic wave. The second bracket accounts for the observed peak in the form function at approximately $x=2$ -4, before the onset of the expected constant value for f at the higher values of x . The bracketed terms have six independent variables and these were obtained by matching the

predictions to the data in the local area where the bracketed terms have maximum influence and then by fine tuning equation (6) to minimizing the mean root-mean-square difference between the predictions and the data. The result was

$$f_e = \frac{x^2 \left(1 - 0.35e^{-((x-1.5)/0.7)^2} \right) \left(1 + 0.5e^{-((x-1.8)/2.2)^2} \right)}{1 + 0.9x^2} \quad (7)$$

This simple expression, given by the solid line in figure 3a, captures the essential features of the data; Rayleigh scattering for $x \ll 1$, the curvature of the data in the region $x=1-5$ and constant in the geometric scattering regime. For small values of x , $f_e = c_0 x^2$, where $c_0 = 1.25$, this value is comparable, though slightly higher, 7%, than the predicted value from equation (5a). For large x , $f_e = 1.1$. Asymptotic expressions for $x \ll 1$, $f_e = 1.25x^2$ and $x \gg 1$, $f_e = 1.1$, are respectively given by the dashed and dotted lines in figure 3a.

For the normalized total scattering cross-section the expression below was used, this is similar to the expression used by Sheng and Hay 1988.

$$\chi = \frac{\beta_1 x^4}{[\xi_1 + \xi_2 x^\kappa + \beta_2 x^4]} \quad (8)$$

Following the approach taken with the form function, for $x \ll 1$, $\chi = (\beta_1/\xi_1)x^4$ and β_1/ξ_1 was obtained from the low x values. For $x \gg 1$, $\chi = \beta_1/\beta_2$, this was obtained from the data. ξ_1 , ξ_2 and κ were then adjusted to minimize the root-mean-square difference between equation (8) and the measurements. The result was

$$\chi_e = \frac{0.29x^4}{[0.95 + 1.28x^2 + 0.25x^4]} \quad (9)$$

As shown in figure 3b, the solid line obtained using equation (9) represents all the main features of the data, with close agreement in the Rayleigh, intermediate and geometric

regimes. For $x \ll 1$, $\chi_e = 0.3x^4$, this is marginally higher than predicted using equation 5(b) by 11%, which is similar to the 7% for the form function in the Rayleigh regime. For $x \gg 1$, $\chi_e = 1.16$, this is comparable with the value for the form function in the geometric scattering regime. $\chi_e = 0.3x^4$ and $\chi_e = 1.16$ are respectively shown by the dashed and dotted lines in figure 3b.

The expressions for the form function and normalized total scattering cross-section in equations (7) and (9) represent all the main features of the observations. To compare the predictions with the observations quantitatively, figure 4 shows plots of f_e , obtained from equation (7) and f , the measurements and χ_e , obtained from equation (9) and χ , the measurements. The solid lines in the figures are $f_e = f$ and $\chi_e = \chi$. It can readily be seen that in both cases the predictions and the observations generally lie along the line of unity gradient over the full range of the measured form function and the normalised total scattering cross-section. To assess the agreement between the predictions and observations a regression equation of the form $y = kz^n$ was applied to the results shown in figure 4. For the form function this gave $f_e = (1.03 \pm 0.04)f^{(1.01 \pm 0.04)}$ with a regression coefficient of 0.98 and for the normalised total scattering cross-section the result was $\chi_e = (1.03 \pm 0.03)\chi^{(1.02 \pm 0.03)}$ with a regression coefficient of 0.99. In both cases, the constant and the indices are not significantly different from unity within the regression uncertainty. Using tabulated values for the regression coefficient (Kennedy and Neville 1976) showed the measured values to be highly significant. Overall the regression analysis shows that equations (7) and (9) accurately represent the magnitude and form of f and χ with x . A similar regression analysis between the observed and predicted values was carried out using the comparable simple expressions of Sheng and Hay 1998 equations (13) and (14), Crawford and Hay 1993 equation (6) and Thorne and Hanes 2002 equations (10a) and (10b). For the form function, the expression of Sheng and Hay 1988 was notably a poorer predictor than equation (7) derived in the present study. The expressions from Crawford and Hay 1993 and Thorne and Hanes 2002 were, however, only marginally poorer predictors than equation (7) and within the error bars of the regression line, although it should be noted that Crawford and Hay does not tend to the Rayleigh solution for $x \ll 1$. For the normalized total scattering cross-section the

expression from Sheng and Hay 1988 was again the poorest predictor, whilst the expression taken from Thorne and Hanes 2002 was comparable to equation (9), though it underestimated the data by about 8% at the higher values of x . On the whole, equation (9) provided the best predictor for the normalized total scattering cross-section.

(iv) Particle size distribution.

Equations (7) and (9) provide the fundamental expressions for f and χ for a suspension of nominally single size; ie with a δ size distribution. These formulations for f and χ need to be evaluated using equations (3) and (4) for use in the marine environment, since the suspended sediments will invariably have a broad size distribution. Therefore allowance has to be made for the impact a range of particle sizes have on $\langle f \rangle$ and $\langle \chi \rangle$. To assess this impact, two particle size distributions were used, the normal, $P_n(a)$ and log-normal $P_{ln}(a)$ distributions. The normal and log-normal distributions are often used to describe the size distributions of sediments collected in the marine environment (Krumbein 1938, Blench 1952, Hardisty, 1990, Soulsby 1997). These can be written as

$$P_n(a) = \frac{1}{\sqrt{2\pi}\sigma} e^{-(a-\langle a \rangle)^2/2\sigma^2} \quad (10)$$

$$P_{ln}(a) = \frac{1}{a\sqrt{2\pi}\zeta} e^{-(\ln(a)-m_o)^2/2\zeta^2} \quad (11)$$

where

$$m_o = \ln\left(\frac{\langle a \rangle^2}{\sqrt{\langle a \rangle^2 + \sigma^2}}\right), \quad \zeta = \sqrt{\ln[(\sigma / \langle a \rangle)^2 + 1]}$$

The mean size of the particles in suspension is given by $\langle a \rangle$ and the standard deviation was set at $\sigma = \kappa \langle a \rangle$, where for all the calculations presented here $\kappa = 0.4$. A value of $\kappa = 0.4$ results in $d_{90}/d_{10} \approx 2$, which represents a moderately well sorted sediment. d_n indicates the grain diameter for which $n\%$ of the grains by mass is finer. Figure 5 shows the two probability distributions for $\langle a \rangle = 100 \mu\text{m}$. The normal distribution is given by the dashed

line and the log-normal distribution by the dotted line. Substituting equations (10) and (11), with equations (7) and (9), into equations (3) and (4), values for $\langle f_e \rangle$ and $\langle \chi_e \rangle$ were calculated and the results are shown in figure 6. The solid line in figures 6a and 6b is f_e and χ_e and the dashed and dotted lines are $\langle f_e \rangle$ and $\langle \chi_e \rangle$ respectively evaluated for normal and log-normal distributions. As can be seen in figure 6, the introduction of a size distribution impacts on both the form function and normalized total scattering cross-section, with the impact being comparable for the two size distributions considered. Simple analytical solutions can be obtained for equation (3) and (4), for the normal distribution in the Rayleigh, $x \ll 1$, and the geometric, $x \gg 1$, scattering regimes. The result for the Rayleigh regime is,

$$\langle f_e \rangle / f_e = \sqrt{\frac{1 + 15\kappa^2 + 45\kappa^4 + 15\kappa^6}{1 + 3\kappa^2}} \quad (12a)$$

$$\langle \chi_e \rangle / \chi_e = \frac{1 + 15\kappa^2 + 45\kappa^4 + 15\kappa^6}{1 + 3\kappa^2} \quad (12b)$$

Equation (12) is shown by the '+' symbol in figure 6. Clearly equation (12) shows that the introduction of a size distribution increases the form function and normalized total scattering cross-section in the Rayleigh regime and the greater the value for κ the larger the effect. In the present case where $\kappa=0.4$, the ratio for $\langle f_e \rangle / f_e = 1.76$ and for $\langle \chi_e \rangle / \chi_e = 3.1$. The impact of the size distribution in this scattering regime is therefore relatively significant. For the geometric regime the ratios are given by,

$$\langle f_e \rangle / f_e = \sqrt{\frac{1 + \kappa^2}{1 + 3\kappa^2}} \quad (13a)$$

$$\langle \chi_e \rangle / \chi_e = \frac{1 + \kappa^2}{1 + 3\kappa^2} \quad (13b)$$

Here the converse is the case, with the introduction of a particle size distribution reducing both the form function and normalized total scattering cross-section, as indicated by the open circles in figure 6. For $\kappa=0.4$ the ratios are $\langle f_e \rangle / f_e = 0.88$ and for $\langle \chi_e \rangle / \chi_e = 0.77$.

Although these changes are not as significant as in the Rayleigh regime, they are not inconsequential.

It is not an objective of the present study to assess the impact the form of $\langle f_e \rangle$ and $\langle \chi_e \rangle$ may have on acoustic estimates of suspended sediment parameters. However, the results in figure 6 do show the importance of having a reasonable estimate for the relative standard deviation, κ . From the results presented here, this estimate may be more important than knowing the precise form of the probability distribution used to represent the particles sizes in suspension.

IV Discussion and conclusion

The present work has sought to provide scattering expressions, for the interpretation of data collected using multi-frequency acoustic backscatter systems, in the study of near bed small-scale sediment transport studies over sandy beds. The use of acoustics for such studies has gained increasing acceptance by sedimentologists and coastal engineers over the past decade or more. To obtain profiles of suspended sediment concentration and particle size, from the backscatter data, requires a description of the acoustic scattering properties of the sediments in suspension. As noted in the text different researchers have used somewhat different expressions to represent the backscattering and attenuating properties of suspensions of sandy sediments. All the expressions are based on sphere scattering, and it is from this acoustic sphere scattering literature, that the definition and nomenclature of using the form function to describe the backscattering characteristics and the normalized total scattering cross-section to represent the attenuation is derived. Because there are no readily available analytical solutions to the scattering by randomly shaped particles, understanding the scattering of suspensions of sand grains has advanced by experimental observation, modifications to the model of sphere scattering and by the use of simple heuristic expressions.

To obtain simple formulation for the scattering properties, all the published data available on scattering by suspensions of sandy sediments were collated. These data have also been augmented by some measurements taken on single irregularly shaped particles. All the data sets were formulated in terms of the form function and normalized total scattering cross-section, so that the results could be directly applied to the interpretation of acoustic backscatter data. The combined data sets had a degree of scatter, and therefore before fitting expressions to the data outliers were identified and rejected. This was followed by smoothing over narrow ranges of x , which highlighted the main features in the data. Simple heuristic expressions, in the form of equations (6) and (8) were put forward which encompassed Rayleigh scattering for $x \ll 1$, and geometric scattering for $x \gg 1$. Using the measurements in the Rayleigh and geometric scattering regimes, some of the constants in

the expressions were established. Other constants were obtained by minimizing the root-mean-square difference between the predictions and the observations. This led to the expressions given in equations (7) and (9). To assess the quality of fit, regression analysis was carried out on the predicted and measured values for the form function and normalized total scattering cross-section. Within the error bars of the regression fit, there was essentially no significant difference between the predicted and observed values. Other formulations for f_e and χ_e were assessed using the regression approach and the expressions of Crawford and Hay 1993 and Thorne and Hanes 2002 were only marginally poorer predictors, although the former does not conform to Rayleigh scattering when $x \ll 1$. To assess the impact a particle size distribution had on f_e and χ_e , equations (3) and (4) were evaluated for normal and log-normal particle size distributions. The calculations showed the effect was significant particularly when $x < 1$. The departure of $\langle f_e \rangle$ and $\langle \chi_e \rangle$ from f_e and χ_e were of sufficient magnitude, that the results indicated the effect of having a particle size distribution should be incorporated into acoustic inversions on acoustic backscatter data collected in the marine environment.

Finally, the aim of the present paper has been to provide those who use acoustics as a tool for studying sediment transport processes, with simple expressions for the scattering properties of suspensions of sandy sediments. Equations (7) and (9) represent a best fit to the published data available at present, with the constraint of Rayleigh scattering for $x \ll 1$ and geometric scattering for $x \gg 1$. These equations, in conjunction with equation (3) and (4), provide a simple basis for interpreting data obtained using multi-frequency ABS over sandy seabeds.

Acknowledgements

This work was supported by NERC UK as part of its small scale sediment process studies. PDT would like to thank ONR USA which partially supported this work under its mine burial programme. RM was support by Kahramanmaras University and the Proudman Oceanographic Laboratory during his visit to the Proudman Oceanographic Laboratory in 2006.

Appendix 1

The aim here is to briefly provide some background on the definitions of the form function and normalized total scattering cross-section. The form function is used to describe the intrinsic scattering properties of the scatterer. Experimentally for a sphere it is defined as

$$f = \frac{2rP_s}{aP_i} \quad (\text{a1})$$

Where, P_i is the pressure incident on the sphere, P_s is the scattered pressure at the receiver at a distance r from the sphere and a is the sphere radius. The factor of 2 is used to give f a value of unity for a rigid sphere in the geometric scattering regime. Essentially r accounts for the spherical spreading of the scattered sound with distance from the sphere, similarly P_i accounts for variations in the incident pressure on the sphere and a normalises the effect of particle size in the geometric scattering regime. This results in a dimensionless parameter directly related to the scattered pressure. For acoustic backscatter transceiver systems it is the scattered pressure in the backscatter direction which is used to obtain f .

The normalised total scattering cross-section is directly related to the sound attenuating properties of the particles in suspension. The change in sound pressure over a distance r in the suspension is given by

$$P_r = P_o e^{-\alpha_s r} \quad (\text{a2})$$

Where P_o is the pressure at a location in the suspension, P_r is the pressure at distance r from P_o in the direction of sound propagation and α_s is the attenuation coefficient of the suspension in Nepers m^{-1} . The attenuation coefficient is given by, $\alpha_s = N\sigma/2$, where N is the number of particles per unit volume and σ is the total scattering cross-section. It is convenient to normalise σ by twice the particles geometric cross-section, $\chi = \sigma/2\pi a^2$, this

is the normalized total scattering cross-section and has a value of unity for a rigid sphere in the geometric scattering regime. Replacing N by the mass concentration and using the definitions for α_s and χ gives

$$\chi = \frac{4\pi\alpha_s}{3M} \quad (\text{a3})$$

As with the form function χ is a dimensionless parameter and is directly related to the attenuating properties of the suspension.

References

- Betteridge, K. F. E., Thorne P. D. and Cooke R. D. 2007. Calibrating multi-frequency acoustic backscatter systems for studying near-bed suspended sediment transport processes. *Continental Shelf Research*. In Press.
- Blench T. 1952. Normal size distribution found in samples of river bed sand. *Civil Engineering*, Vol 22, No 2, 147.
- Chinnery, P. A. Humphrey V. F. and Zhang J. 1997. Low-frequency acoustic scattering by a cube. Experimental measurements and theoretical predictions. *J. Acoust Soc Amer.* 101, 2571-2582, 1997.
- Clay C. S. and Medwin H. 1997. *Acoustical Oceanography: Principles and applications*. Published by John Wiley & Sons USA.
- Crawford, A.M., Hay, A.E., 1993. Determining suspended sand size and concentration from multifrequency acoustic backscatter. *J. Acoust. Soc. Am.* 94(6), 3312-3324.
- Dohmen-Janssem C. M and Hanes D. M. 2005. Sheet flow and suspended sediment due to wave groups in a large wave flume. *Cont. Shelf Res.*, 25, 333-347.
- Flammer G. H. 1962. Ultrasonic measurements of suspended sediments. *Geological Survey Bulletin No 1141-A*, United States Government Printing Office, Washington.
- Green M. O. Vincent C. E. and Trembanis A. C. 2004. Suspension of coarse and fine sand on a wave-dominated shoreface, with implications for the development of rippled scour depressions *Cont. Shelf Res.*, 24, 317-335.
- Hardisty J. 1990. *Beaches form and process*. Published by Unwin Hyman London
- Hay A. E. 1991. Sound scattering from a particle-laden turbulent jet, *J. Acoust Soc. Am.*, 90, 2055-2074.
- Hay, A.E., Sheng. J., 1992. Vertical profiles of suspended sand concentration and size from multifrequency acoustic backscatter. *J. Geophys. Res.* 97(C10). 15661-15677.
- He C and Hay A. E. 1993. Broadband measurements of the acoustic scattering cross section of sand particles in suspension. *J. Acoust. Soc. Am.* 94(4) 2247-2254.
- H C van de Hulst. 1981 'Light scattering by small particles'. New York, Dover Publications. pp470.

- Jansen, R.H. J., 1978. The in-situ measurement of sediment transport by means of ultrasound scattering. A Delft Hydraulics Laboratory report, The Netherlands, publication number 203, pp13.
- Jansen, R.H. J., 1979. An Ultrasonic Doppler Scatterometer for Measuring Suspended Sand Transport, in Ultrasonic International 79, Conference Proceedings, edited by Z. Novak (Graz, Austria), UI 79,. 366-371.
- Kennedy J. B. and Neville A. M. 1976. Basic statistical methods for engineers and scientists. Published by Dun-Donnelley publishers. pp 490
- Krumbein W. C. 1938. Size frequency distribution of sediments and the normal phi curve. J Sediment Petrol Vol 8, No 3, 84-90,
- Libicki, C., Bedford, K.W., Lynch, J.F., 1989. The interpretation and evaluation of a 3-MHz acoustic backscatter device for measuring benthic boundary layer sediment dynamics, J. Acoust. Soc. Am. 1501-1511.
- Neubauer W. G., Vogt R. H. and Dragonette L R .1974. Acoustic reflection from elastic spheres. 1 Steady-state signals. J. Acoust Soc Am. Vol 55, No 6, 1123-1129.
- Schaafsma A. S. and Hay A. E. 1997. Attenuation in suspensions of irregularly shaped sediment particles: A two-parameter equivalent spherical scatterer model. J. Acoust. Soc. Am. 102, 1485-1502.
- Schaafsma, A.S., and der Kinderen, W.J.G.J., 1985. Ultrasonic instruments for the continuous measurement of suspended sand transport. Proceedings of the IHAR symposium on Measuring Techniques in Hydraulic Research (editor A.C.E Wessels) held at Delft Hydraulics 22-24 April 1985 and published by A. A. Balkema Rotterdam in 1986. 125-136.
- Sheng, J. and Hay A. E. 1988. An examination of the spherical scatterer approximation in aqueous suspensions of sand. J. Acoust. Soc. Am. 83, 598-610.
- Soulsby, R., 1997. Dynamics of Marine Sands. Thomas Telford Publications, London.
- Thorne, P. D. Hardcastle, P. J. and Soulsby, R.L. 1993. Analysis of acoustic measurements of suspended sediments, J. of Geophysical Res., Vol. 98, No. C1, 899-910.
- Thorne P. D., Waters, K.R. and Brudner, T.J. 1995. Acoustic measurements of scattering by objects of irregular shape. J. Acoust. Soc. of Am., 97(1), 242-251.

Thorne P.D. and Hanes, D. M. 2002. A review of acoustic measurement of small scale sediment processes. *Continental Shelf Res.* 22, 603-632.

Thorne P. D. Williams, J. J. and Davies, A. G. 2002. Suspended sediments under waves measured in a large scale flume facility. *J. Geophysical Research.* Vol 107, No C8, 10.1029/2001JC000988. 4.1-4.16.

Thorne P. D. and Buckingham M. J. 2004. Measurements of scattering by suspensions of irregularly shaped sand particles and comparison with a single parameter modified sphere model. *J. Acoust Soc Amer.* 116 (5) 2876-2889.

Van de Hulst H. C. 1981. *Light scattering by small particles.* Published by Dover, New York.

Vincent C. E. and Hanes D. M. 2002. The accumulation and decay of near-bed suspended sand concentration due to waves and wave groups. *Cont. Shelf Res.*, 22, 1987-2000.

Figure captions

Figure 1. a) Measurements of the form function, f , from; Hay 1991 (Δ), He and Hay 1993 (*), Thorne et al 1995 (o) and Thorne and Buckingham 2004 (\bullet). b) Measurements of the normalized total scattering cross-section, χ , from; Flammer 1962 (x), Sheng and Hay 1988 (*) (using the data of Jansen 1978, 1979 and Schaafsma and der Kinderen 1985), Hay 1991 (Δ), Schaafsma and Hay 1997 (o) and Thorne and Buckingham 2004 (\bullet). The solid lines are linear regression fits to the logarithm of the data for $x \leq 2.5$ and $x > 2.5$.

Figure 2. a) Plot of the ratio of the measured form function, f , to the form function calculated from the regression lines in figure 1a, f_r . b) Plot of the ratio of the measured normalized total scattering cross-section, χ , to the normalized total scattering cross-section calculated from the regression lines in figure 1b, χ_r . The two horizontal lines represent ratios equal to 1.5^{-1} and 1.5. The symbols used in figure 2 correspond with those used in figure 1 and their associated data sets.

Figure 3. a) Measurements of the filtered and smoothed form function (o), equation (7) (---), Rayleigh scattering (---) and geometric scattering (---). b) Measurements of the filtered and smoothed normalized total scattering cross-section (o), equation (9) (---), Rayleigh scattering (---) and geometric scattering (---).

Figure 4. a) Regression plot of the predicted form function from equation (7), f_e , against the measured form function f . The solid line is $f_e = f$. b) Regression plot of the predicted normalized total scattering cross-section from equation (9), χ_e , against the measured normalized total scattering cross-section, χ . The solid line is $\chi_e = \chi$.

Figure 5. Normal probability distribution (---) and log-normal probability distribution (---), for $\langle a \rangle = 100 \mu\text{m}$ and $\sigma(a) = 0.4 \langle a \rangle$.

Figure 6. a) Plots of the form function from equation (7), f_e (---), and from equation (3), $\langle f_e \rangle$. b) Plots of the normalized total scattering cross-section from equation (9), χ_e (---), and from equations (4), $\langle \chi_e \rangle$. P(a) was given by a normal distribution (---) and a log-

normal distribution (\cdots), with $\sigma(a)=0.4\langle a \rangle$. Also shown are the normal distribution analytical solutions for $\langle f_e \rangle$ and $\langle \chi_e \rangle$ in the Rayleigh (+) and geometric (o) scattering regimes.

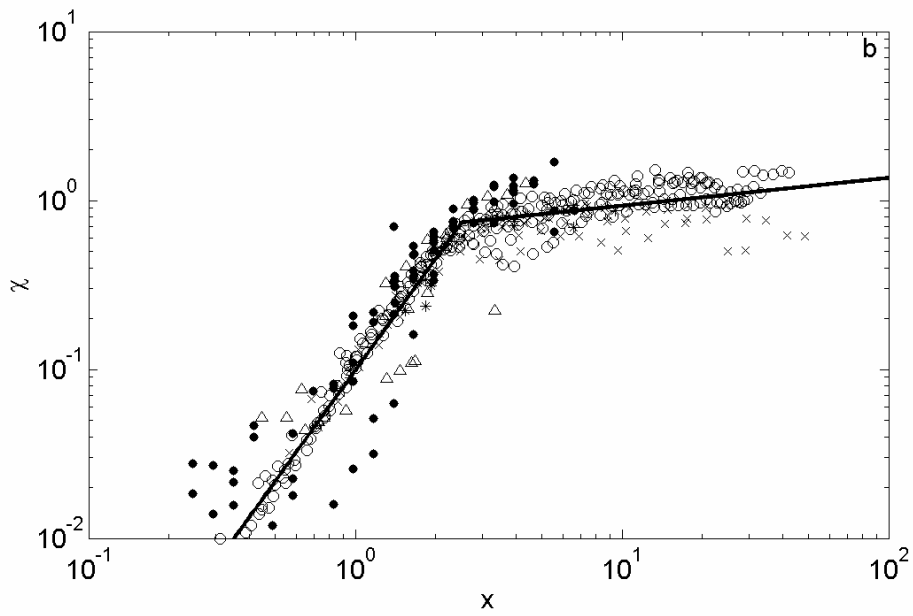
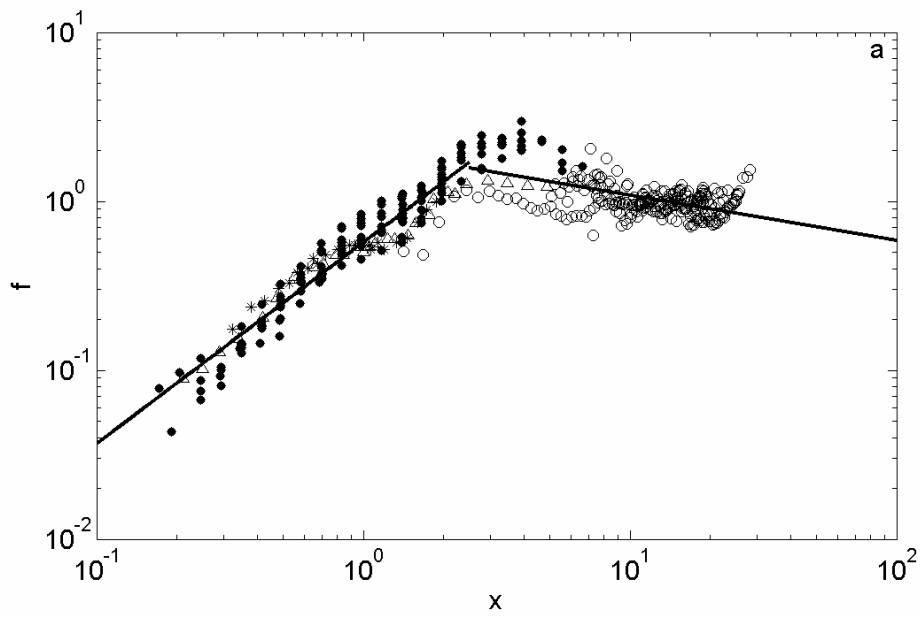


Fig 1 n:\mat5work\labscatter\results\ramazan\form_chi_report_pdt.m

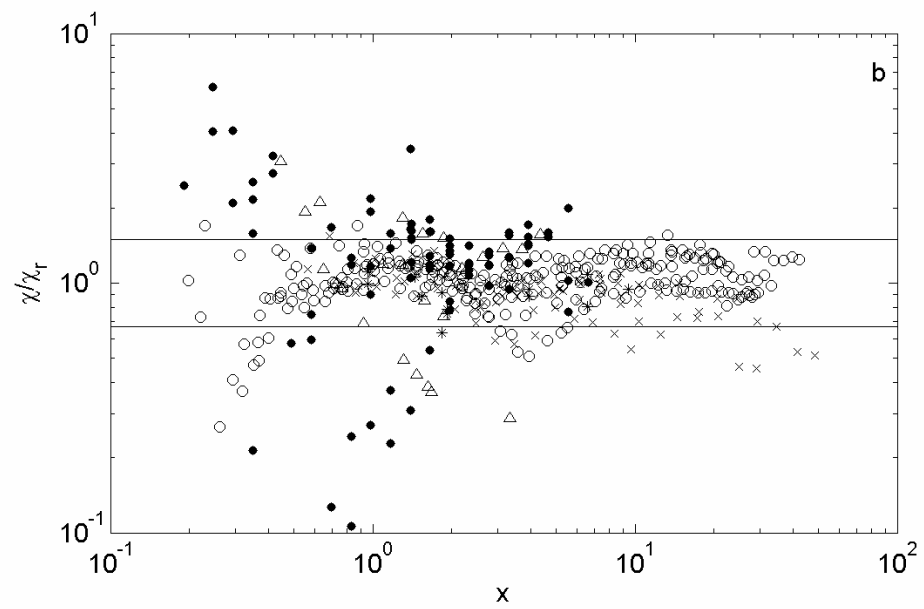
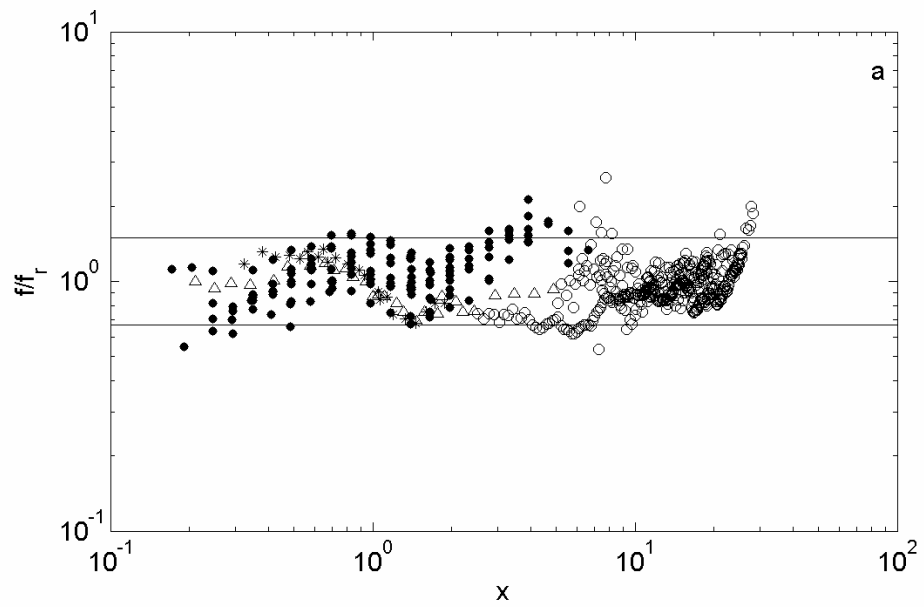


Fig 2 n:\mat5work\labscatter\results\ramazan\form_chi_report_pdt.m

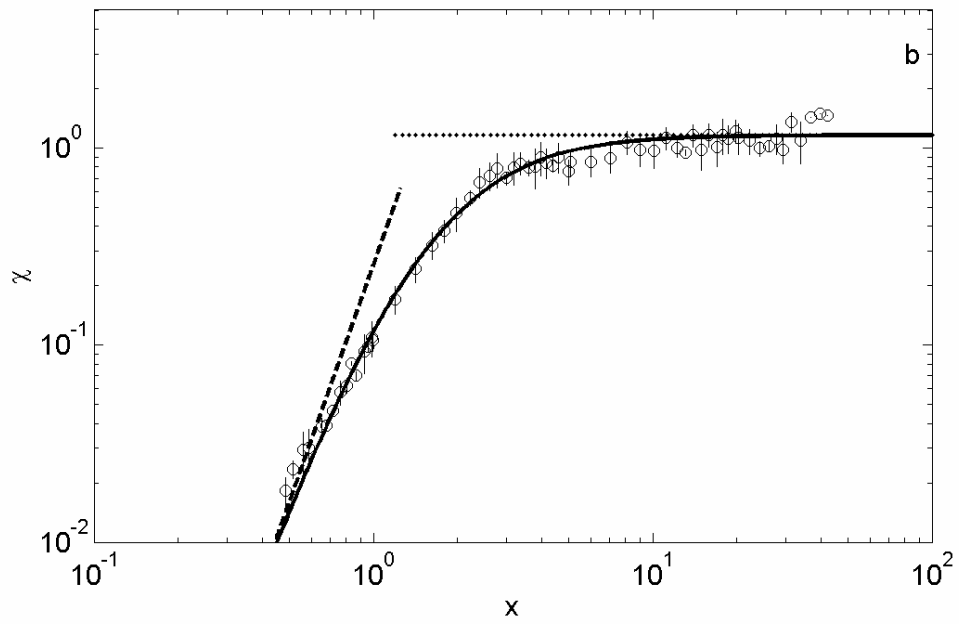
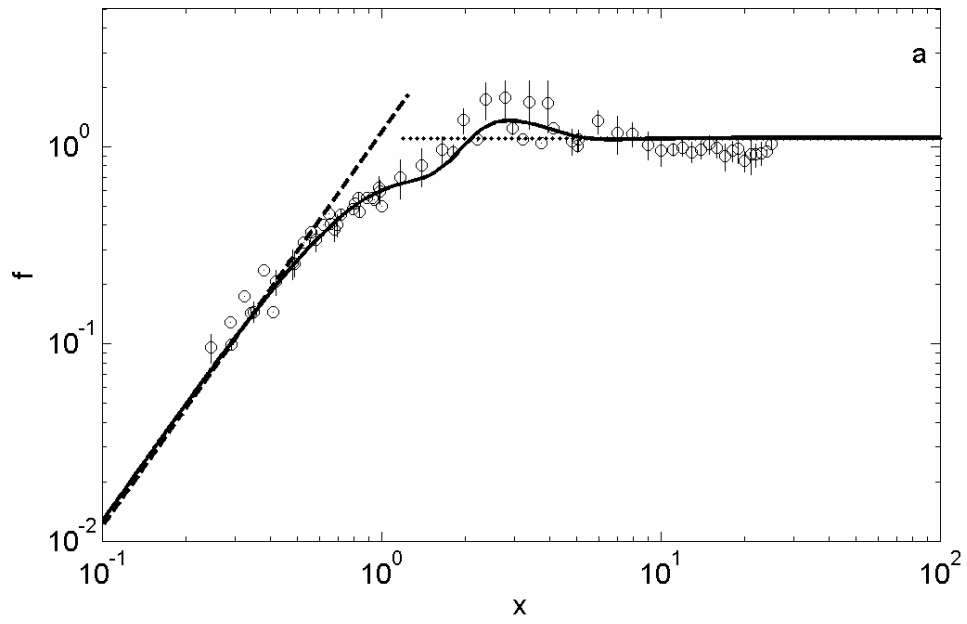


Fig 3 n:\mat5work\labscatter\results\ramazan\form_chi_report_pdt.m

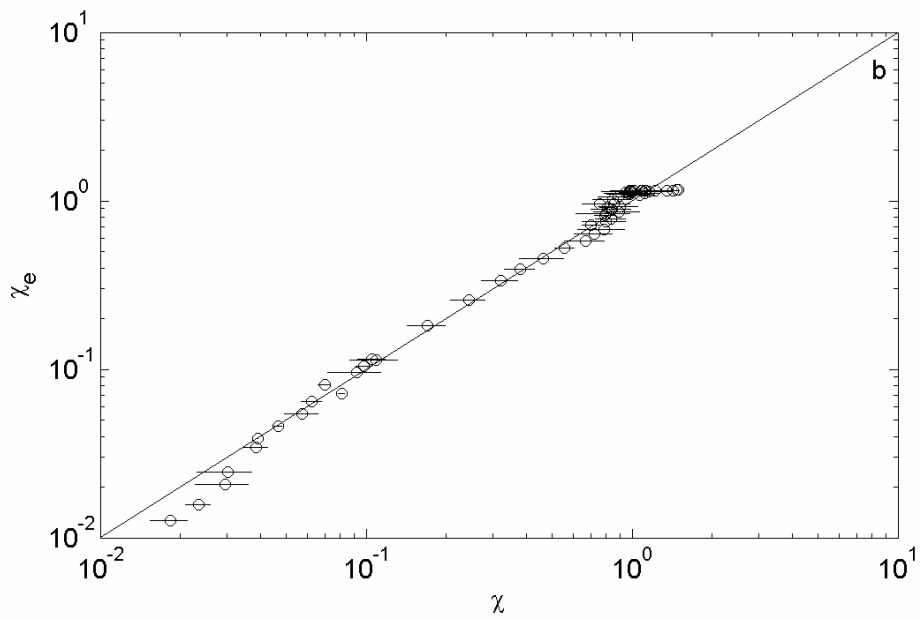
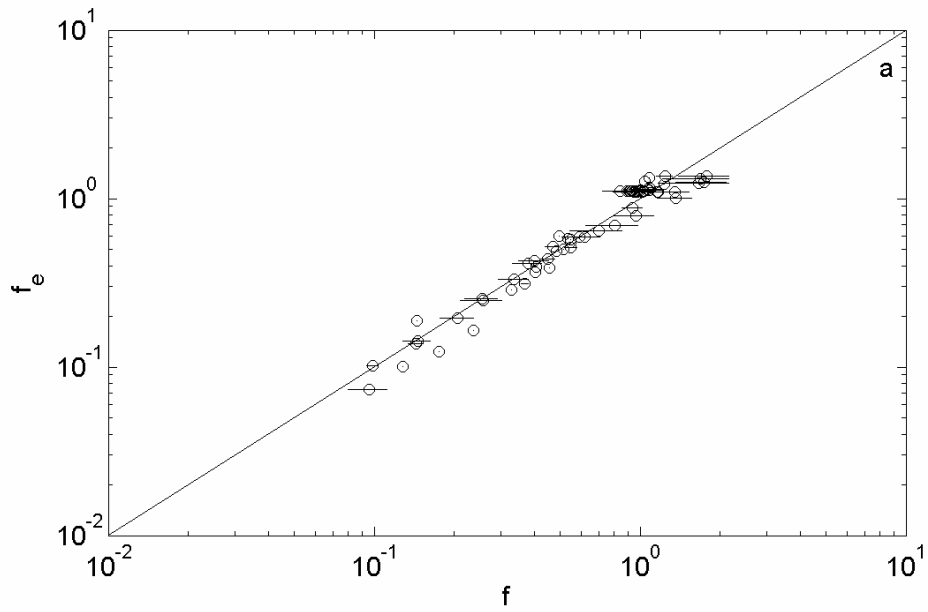


Fig 4 n:\mat5work\labscatter\results\ramazan\form_chi_report_pdt.m

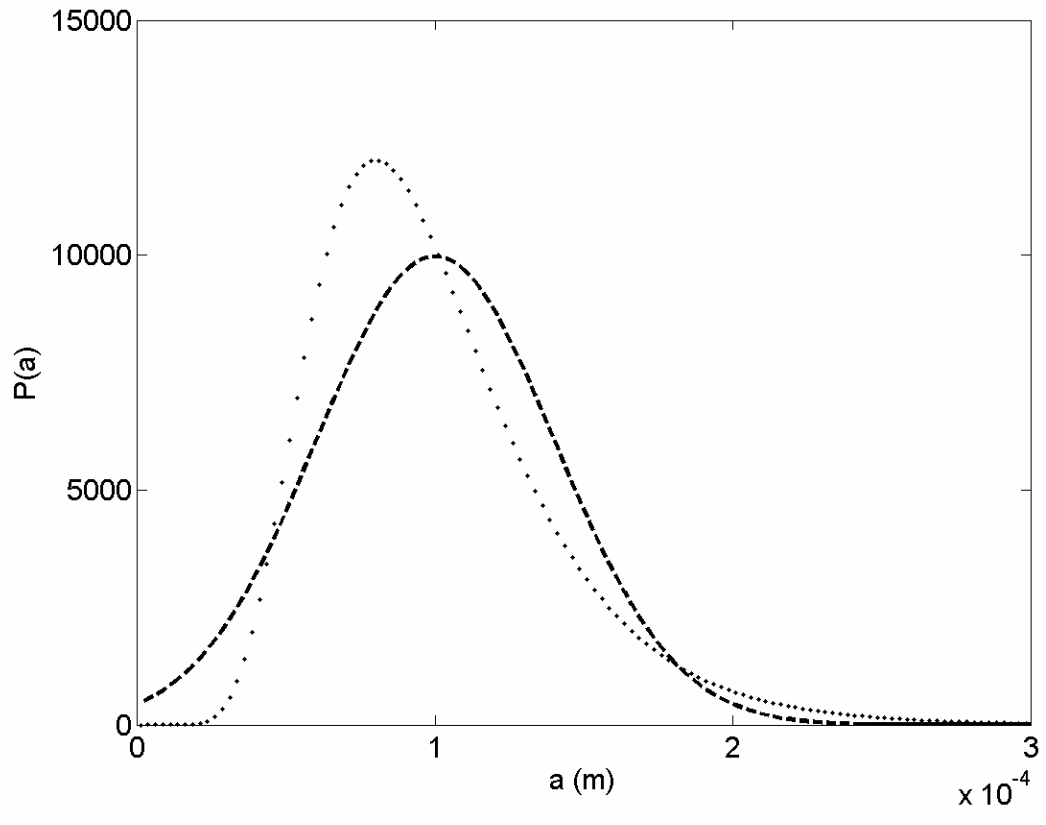


Fig 5 n:\mat5work\labscatter\results\ramazan\av_chi_fm.m

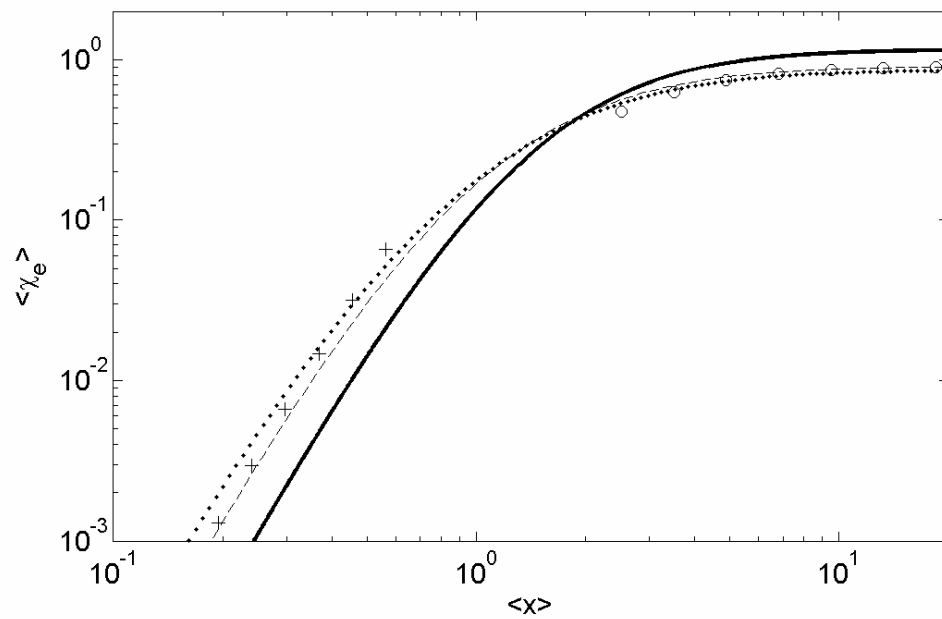
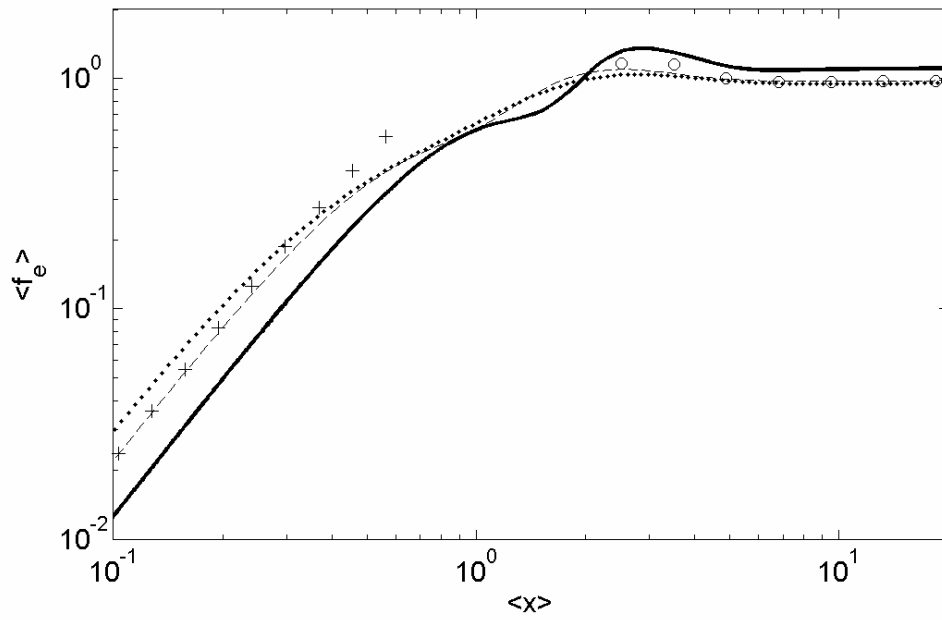


Fig 6 n:\mat5work\labscatter\results\ramazan\av_chi_fm.m